

submitted to *Global Biogeochemical Cycles*, February 20, 2004, revised manuscript August 17, 2004

Interannual variability of the upper ocean carbon cycle at station ALOHA near Hawaii

Holger Brix and Nicolas Gruber

IGPP & Department of Atmospheric and Oceanic Sciences, University of California, Los Angeles.

Charles D. Keeling

Scripps Institution of Oceanography, University of California, La Jolla.

Abstract. We investigate interannual variability of the upper ocean carbon cycle in the subtropical North Pacific on the basis of a fourteen year time-series (1988-2002) of carbon parameters from Station ALOHA, the site of the U.S. JGOFS Hawaii Ocean Time-series program (HOT). The data reveal substantial interannual variability in near surface concentrations of dissolved inorganic carbon normalized to constant salinity ($sDIC$, peak-to-peak amplitude of $\pm 4 \mu\text{mol kg}^{-1}$), computed ocean surface partial pressure of CO_2 ($p\text{CO}_2$, $\pm 6 \text{ ppm}$), and the $^{13}\text{C}/^{12}\text{C}$ ratio of DIC ($\pm 0.07\text{‰}$). A strong anti-correlation ($r = -0.50$) between interannual anomalies in sea-surface temperature (SST) and $sDIC$ is found, which tends to suppress the correlation of either of these properties with $p\text{CO}_2$. In contrast, no significant correlation ($p < 0.05$) is found between anomalies of the $^{13}\text{C}/^{12}\text{C}$ ratio of DIC and any other parameter. A diagnostic box model analysis reveals that interannual variability of near surface ocean $sDIC$ is driven by air-sea gas exchange, net community production, and lateral transport. In warmer than normal years the seasonal carbon cycle tends to be weakened, with a $sDIC$ reduction in the mixed layer caused by diminished gas exchange and lateral transport outweighing the effect of less intense $sDIC$ removal by net community production. This explains the observed anti-correlation between SST and $sDIC$. Interannual (peak-to-peak) variability of air-sea gas exchange ($\pm 0.4 \text{ mol m}^{-2} \text{ yr}^{-1}$, i.e. 40% of the annual mean value) is primarily governed by strongly co-varying changes in SST and wind speeds. Net community production varies interannually by up to $\pm 0.9 \text{ mol m}^{-2} \text{ yr}^{-1}$ (39%) and tends to be associated with changes in horizontal transport. Less than 20% of the interannual variance in $sDIC$ near Hawaii can be explained by the Pacific Decadal Oscillation (PDO), and an even smaller fraction (less than 5%) by the El Niño-Southern Oscillation (ENSO). Because SST variations over a sizable fraction of the North Pacific subtropical gyre vary in concert with those at Sta. ALOHA, it is plausible that air-sea fluxes in this region vary also synchronously, resulting in a variability of the atmospheric CO_2 sink strength of the North Pacific subtropical gyre of up to $\pm 0.2 \text{ PgC yr}^{-1}$.

1. Introduction

The increase of atmospheric CO₂ is not steady, but shows substantial fluctuations from year to year [Bacastow, 1976; Conway *et al.*, 1994; Keeling *et al.*, 1995]. These anomalies, which range up to $\pm 2 \text{ PgC yr}^{-1}$ ($1 \text{ PgC} = 10^{15} \text{ gC}$), are not driven by interannual variations in fossil fuel emissions, as these variations are generally much less than 1 PgC yr^{-1} [Houghton *et al.*, 2001; Sarmiento and Gruber, 2002]. This indicates that the natural carbon cycle is far from being balanced over the annual cycle, but that substantial amounts of carbon are exchanged anomalously between the ocean, terrestrial biosphere, and the atmosphere from year to year. Although Bacastow [1976] pointed out already nearly 30 years ago that these interannual variations in the atmospheric CO₂ growth rate are correlated with the El Niño/Southern Oscillation (ENSO) phenomenon [Philander, 1990], the magnitude and spatial pattern of these anomalous fluxes and the mechanisms driving them are still not well understood [Heimann, 1995; Quay, 2002].

Atmospheric budget considerations (e.g. Francey *et al.* [1995], Keeling *et al.* [1995]), inversions of atmospheric CO₂ concentrations (e.g. Bousquet *et al.* [2000] and Rödenbeck *et al.* [2003]), as well as modeling studies of the land biosphere (e.g. Kindermann *et al.* [1996], Cramer *et al.* [2001], and Sitch *et al.* [2003]) and of the ocean (e.g. Winguth *et al.* [1994], Le Quéré *et al.* [2000], and McKinley [2002]) have been applied to determine the relative roles of the ocean and land biosphere in contributing to anomalous CO₂ fluxes and to estimate how these fluxes are distributed around the globe (for a summary see also Peylin *et al.* [2004]). Keeling *et al.* [1995], using concurrent observations of the concentration and ¹³C/¹²C ratio of atmospheric CO₂ and an isotopic budget calculation, found large anomalous fluxes for both the ocean and the terrestrial biosphere with a peak-to-peak amplitude of up to $\pm 2.5 \text{ PgC yr}^{-1}$. Francey *et al.* [1995], employing a similar technique but their own atmospheric data, came to rather different conclusions. They estimated that nearly all the variability observed in atmospheric CO₂ is driven by the land biosphere. Recent studies relying on the distribution of atmospheric CO₂ and/or the isotopic composition of CO₂ to invert for the magnitude and spatial pattern of CO₂ fluxes at earth's surface find a relative contribution in between these two extremes, with the variability of the land biosphere contributing about twice as strongly to the total variability as the ocean [Rayner *et al.*, 1999; Bousquet *et al.*, 2000; Baker, 2001; Rödenbeck *et al.*, 2003].

All ocean modeling studies conducted so far show a very small contribution of the ocean carbon cycle to atmospheric CO₂ variability [Winguth *et al.*, 1994; Le Quéré *et al.*, 2000; McKinley, 2002], with a maximum contribution of less than $\pm 0.5 \text{ PgC yr}^{-1}$. These ocean modeling studies also indicate that the variability in the air-sea CO₂ fluxes is dominated by the Equatorial Pacific and driven by the large-scale changes in ocean dynamics associated with ENSO. During a positive phase of ENSO (i.e. El Niño), upwelling of highly CO₂ supersaturated waters to the surface in the eastern equatorial Pacific is suppressed, resulting in a reduction of the strong outgassing of CO₂ that is typical for this region [Keeling *et al.*, 1989; Feely *et al.*, 1999; Chavez *et al.*, 1999; Le Quéré *et al.*, 2000; McKinley, 2002]. During a negative phase of ENSO (i.e. La Niña), upwelling is particularly strong, making this region an anomalous source of CO₂ to the atmosphere. In situ observations [Feely *et al.*, 1999; Chavez *et al.*, 1999], and the results from oceanic modeling studies [Le Quéré *et al.*, 2000; McKinley, 2002], as well as those from atmospheric CO₂ inversions [Bousquet *et al.*, 2000] agree generally on the magnitude and timing of the anomalous fluxes of CO₂ in this region [Peylin *et al.*, 2004]. These studies show that the variability of air-sea CO₂ fluxes from this region does not exceed $\pm 0.4 \text{ PgC yr}^{-1}$, i.e. only about 20% of the observed interannual variations in atmospheric CO₂. The phase of the anomalous air-sea CO₂ fluxes from the equatorial Pacific tends to be opposite of the observed atmospheric anomalies.

Given the large area of the extra-tropical oceans, relatively small anomalies in the air-sea CO₂ fluxes in these regions can lead to substantial variations in atmospheric CO₂. In contrast to the equatorial regions, the different methods to estimate the magnitude of interannual variability in air-sea CO₂ fluxes give rather different results in the extra-tropical regions [Peylin *et al.*, 2004]. Current ocean models simulate a small interannual variability, with a strong tendency for the different basins to compensate each other [Le Quéré *et al.*, 2000; McKinley, 2002]. Atmospheric CO₂ inversions suggest, on the other hand, much higher air-sea CO₂ flux variability [Bousquet *et al.*, 2000].

No in situ data exist on basin-wide scales to evaluate these results. However, two long-term upper ocean carbon time-series exist in the subtropical gyres that permit us to gain insight into interannual variability in the extra-tropical ocean carbon cycle on a regional scale. These two time-series were established as part of the U.S. Joint Ocean Global Flux Study (JGOFS) program: one near Bermuda (Bermuda At-

lantic Time-Series (BATS)), building on the long running time-series from Hydrostation "S" [Michaels and Knap, 1996], and one near Hawaii (Hawaii Ocean Time-series (HOT) program [Karl and Lukas, 1996]). Both JGOFS time-series programs are operating since 1988 [Lomas *et al.*, 2002]. Interannual variability of the oceanic carbon cycle near Bermuda was addressed already by several studies [Bates *et al.*, 1996; Bates, 2001; Bates *et al.*, 2002; Gruber *et al.*, 2002], while most carbon cycle studies at HOT focused on long-term trends [Winn *et al.*, 1998; Dore *et al.*, 2003; Keeling *et al.*, 2004]. As a consequence, relatively little is known about the magnitude of interannual variability in the upper ocean carbon cycle near Hawaii and the processes that control it.

Interannual variability in the upper ocean carbon cycle near Bermuda is mainly controlled by the strength of winter time convection [Bates, 2001; Gruber *et al.*, 2002]. Because DIC and nutrients increase with depth, winters with deeper convection tend to entrain more DIC and nutrients into the mixed layer. For those winters, Gruber *et al.* [2002] reported enhanced biological production (likely fueled by elevated nutrient availability) and increased uptake of CO_2 from the atmosphere, a result of both stronger wind speeds and cooler sea-surface temperatures (SST) that lower oceanic pCO_2 . Such winters tend to be associated with negative phases of the North Atlantic Oscillation (NAO), suggesting that interannual variations seen near Bermuda might be congruent with variations across the entire subtropical gyre of the North Atlantic.

In the Pacific at Sta. ALOHA, mixed layer depth variability is substantially smaller than near Bermuda and therefore has a smaller impact on the upper ocean carbon cycle [Keeling *et al.*, 2004]. It is currently unknown, which other forcing factor is dominant in controlling interannual variability of the upper ocean carbon cycle near Hawaii. One possibility are variations in SST, which could force variations in air-sea gas exchange through their impact on solubility. SST anomalies tend to vary in concert with ENSO across large regions of the Pacific [Kawamura, 1994] due to the strong forcing from the equatorial Pacific, either directly or through teleconnections [Bjerknes, 1969]. However, SST anomalies near Hawaii are only weakly correlated with ENSO. The Pacific Decadal Oscillation (PDO, Mantua *et al.* [1997]; Mantua and Hare [2002]) constitutes another important climate mode in the North Pacific. The impact of this interannual mode on surface meteorology near Hawaii, though, is also relatively small.

In order to investigate the impact of PDO and ENSO and that of interannual variability of meteorological forcing on the upper ocean carbon cycle near Hawaii in general, we analyze an inorganic carbon data set based on water samples taken from the mixed layer at Sta. ALOHA and measured in the laboratory by the Carbon Dioxide Research Group at the Scripps Institution of Oceanography [Keeling *et al.*, 2004]. This dataset together with other independent data (e.g. from the HOT program [Lukas and Karl, 1999]) permits us to apply a diagnostic box model [Gruber *et al.*, 1998; Keeling *et al.*, 2004], which quantifies the main processes controlling the upper ocean carbon cycle balance. A brief outline of this model is given in section 3. The analysis and discussion of the model output and a statistical analysis of the results is presented in section 4. In section 5 we compare our results to independent estimates of air-sea gas exchange and carbon export. In section 6, we discuss the relationship of interannual variability at Sta. ALOHA with large-scale modes of climate variability and also compare our results with those obtained near Bermuda highlighting similarities and differences between these two subtropical timeseries sites. We also further discuss the role of the subtropical oceans for the atmospheric CO_2 budget. In the final section, we summarize our results.

2. Observations

The dataset employed in this study is discussed in detail by Keeling *et al.* [2004] with an emphasis on seasonal cycles and long term trends. Figure 1a-b shows the time-series for sea-surface temperature (SST) and sea-surface salinity (SSS). The concentration of dissolved inorganic carbon in the upper ocean normalized to a constant salinity of 35 ($s\text{DIC}$) is depicted in Figure 1c and the $^{13}\text{C}/^{12}\text{C}$ ratio of DIC (referred to as the reduced isotopic ratio $\delta^{13}\text{C}$) is plotted in Figure 1d. Figure 1e shows the partial pressure of CO_2 in seawater (pCO_2), calculated from DIC, Alk , temperature, salinity, and nutrients [Keeling *et al.*, 2004]. The thick line in Figure 1e depicts atmospheric pCO_2 ($\text{pCO}_2^{\text{atm}}$), computed from measured atmospheric CO_2 mixing ratios at Cape Kumakahi (Keeling *et al.* [1989] and updates).

Distinct seasonal cycles for $s\text{DIC}$, $\delta^{13}\text{C}$, and computed pCO_2 can be found in the upper ocean near Hawaii, whereas $s\text{Alk}$ (not shown) exhibits only short-term drawdowns (see detailed discussion by Keeling *et al.* [2004]). The partial pressure of CO_2 and $s\text{DIC}$ show long-term increases over the duration of our records, $\delta^{13}\text{C}$ a long-term decrease. These trends can mostly be

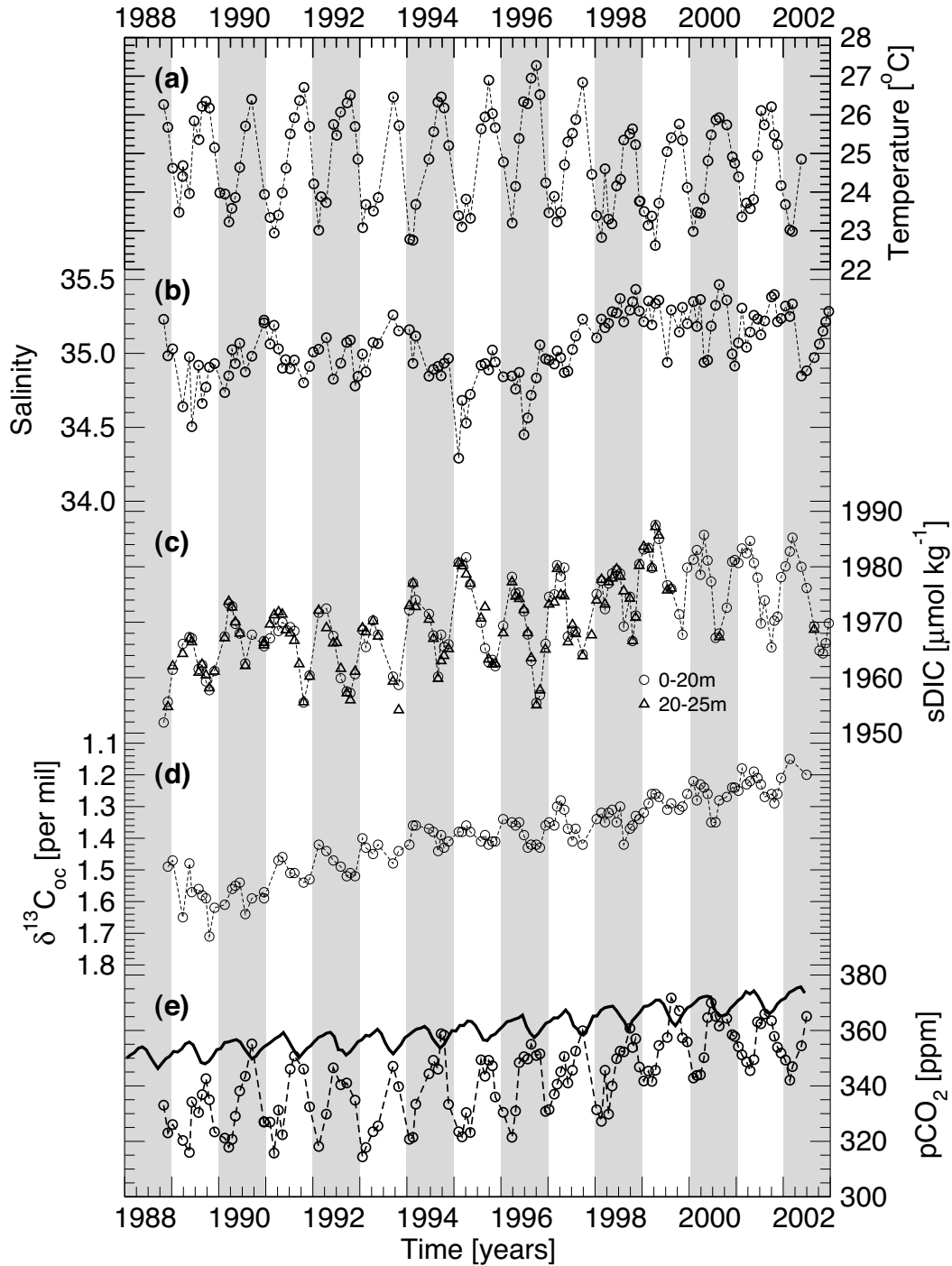


Figure 1. Time-series of upper ocean properties at station ALOHA from 1988 to 2002. (a) Sea surface temperature; (b) Sea surface salinity; (c) Dissolved inorganic carbon ($sDIC$) normalized to a salinity of 35.0, (d) $\delta^{13}C$ of DIC (inverted scale). (e) Oceanic pCO_2 calculated from DIC, Alk , temperature, salinity, and inorganic nutrients (see text). In (e) the solid line shows atmospheric pCO_2 computed from monthly mean xCO_2 data measured at Cape Kumakahi (see text). Open circles denote samples taken at approx. 5 m depth, while open triangles denote samples taken at approx. 25 m depth. SST and SSS are from the HOT core program [Lukas and Karl, 1999]; all other data are from the Carbon Dioxide Research Group at the Scripps Institution of Oceanography [Keeling et al., 2004].

attributed to the uptake of isotopically light anthropogenic CO_2 from the atmosphere. Trends in $s\text{DIC}$ and $p\text{CO}_2$ appear to be also a result of a change in SSS around 1996/1997 (see Figure 1b) [Dore *et al.*, 2003; Keeling *et al.*, 2004], causing an increase in alkalinity, which tended to induce an increase in DIC so as to maintain a constant partial pressure of CO_2 (termed dilution effect, see Keeling *et al.* [2004]). As it takes about a year to equilibrate DIC in a 50 m deep surface mixed layer with atmospheric CO_2 , the surface ocean CO_2 system at Sta. ALOHA has not been able to fully equilibrate with atmospheric CO_2 in response to this surface Alk perturbation, leading to elevated surface ocean $p\text{CO}_2$ trends as well. According to Dore *et al.* [2003] the salinity increase after 1996/1997 was primarily a result of a dramatic reduction in local precipitation. Keeling *et al.* [2004] suggested that the salinity change might also be the result of a change in water mass near Sta. ALOHA, and that this change might be associated with a recent sign reversal of the PDO [Chavez *et al.*, 2003; Peterson and Schwing, 2003].

In order to focus on the interannual variability component of our time-series, we removed from them mean seasonal cycles and trends. This was accomplished by fitting a linear function and harmonic functions of 12, 6, and 4 month periods to the data using the method of least squares and then computing residuals. The resulting anomaly time-series of SST, SSS, $s\text{Alk}$, $s\text{DIC}$, $\delta^{13}\text{C}$, and $p\text{CO}_2$ are displayed in Fig. 2 together with smoothing spline fits [Enting, 1987] with a cut-off period of about one year to emphasize interannual variability. Actual values for interannual variability here and in the following are addressed as peak-to-peak.

Warm (positive) SST anomalies (Fig. 2a) existed in 1991/1992, 1995 to 1997, and in 2000/2001 with maxima in the spline fits of up to 0.5°C , while cold anomalies prevailed from 1989 to 1991, 1993 to 1995, and 1998/1999. Anomalies of SSS are dominated by a drop in 1994 and a strong increase in 1996/1997 (Fig. 1b and Fig. 2b). $s\text{Alk}$ anomalies (Fig. 2c) follow the phasing of SSS very closely with values of $\pm 15 \mu\text{mol kg}^{-1}$. Anomalies of $s\text{DIC}$ reach values of $\pm 5 \mu\text{mol kg}^{-1}$ compared to its mean seasonal amplitude of $15 \mu\text{mol kg}^{-1}$ (Fig. 2d). Interannual anomalies of $\delta^{13}\text{C}$ (Fig. 2e) reach values of $\pm 0.07\text{‰}$, more than half of the amplitude of the seasonal cycle (0.10‰). Interannual variability of $p\text{CO}_2$ is also distinct (Fig. 2f) with anomalies of $\pm 6 \text{ ppm}$, compared to a seasonal amplitude of 20 ppm.

In regard to interannual anomalies (see Table 1) SST and SSS are negatively correlated (linear correlation coefficient, $r = -0.49$). Positive SST anomalies tend to

coincide with negative $s\text{DIC}$ anomalies and vice versa ($r = -0.50$). This negative correlation leads to a suppression of the correlation of either with surface ocean $p\text{CO}_2$ (Fig. 2f), because any increase in $p\text{CO}_2$ resulting from a positive SST anomaly tends to be offset by a decrease in $p\text{CO}_2$ resulting from a negative DIC anomaly. A similar canceling effect exists for the seasonal cycle of $p\text{CO}_2$ [Keeling *et al.*, 2004], whereby SST dominates over the impact of DIC. By contrast, the impact of $s\text{DIC}$ anomalies tend to prevail over SST anomalies on interannual time-scales, leading to a stronger correlation of $s\text{DIC}$ with $p\text{CO}_2$ ($r = +0.42$ compared to $r = +0.16$ for SST). This is especially the case in autumn (defined here as August through November: ASON), when the correlation between $s\text{DIC}$ and $p\text{CO}_2$ is $r = +0.73$. In spring/summer (April through July: AMJJ) the impact of SST dominates, while in winter (December through March: DJFM) the impact of SST and $s\text{DIC}$ anomalies nearly cancel, yielding negligible correlations.

The influence of SSS on Alk is reflected in the high correlation between the two quantities ($r = +0.89$), SSS and DIC show an even higher positive correlation ($r = +0.94$). DIC and Alk have opposite effects on $p\text{CO}_2$, which explains the small and not significant correlation of SSS with $p\text{CO}_2$ ($r = +0.26$). Salinity therefore has only a small influence on interannual variability of $p\text{CO}_2$ at Sta. ALOHA, although we have shown that it is of importance for explaining changes in long-term trends [Keeling *et al.*, 2004]. It is interesting to note that salinity normalized alkalinity, $s\text{Alk}$, is negatively correlated with SSS ($r = -0.40$, also compare Figs. 2b and c). The connection between the two quantities cannot be due to freshwater fluxes as these would actually lead to a positive correlation. We therefore interpret this correlation to reflect changes in water masses, consistent with a global scale negative correlation between SSS and surface $s\text{Alk}$ [Gruber *et al.*, 1999].

Correlations of $\delta^{13}\text{C}$ with other quantities are generally not significant at the 95% confidence level.

3. The diagnostic model

We apply a diagnostic box model to deduce the processes causing the observed interannual variability of the upper ocean carbon cycle near Hawaii. The model is based on the work of Gruber *et al.* [1998] and was employed by Gruber and Keeling [1999], Gruber *et al.* [2002] and Keeling *et al.* [2004]. A conceptually similar model was used by Quay and Stutsman [2003]. The model setup used for the present study is described in detail by Keeling *et al.* [2004]. We confine ourselves here

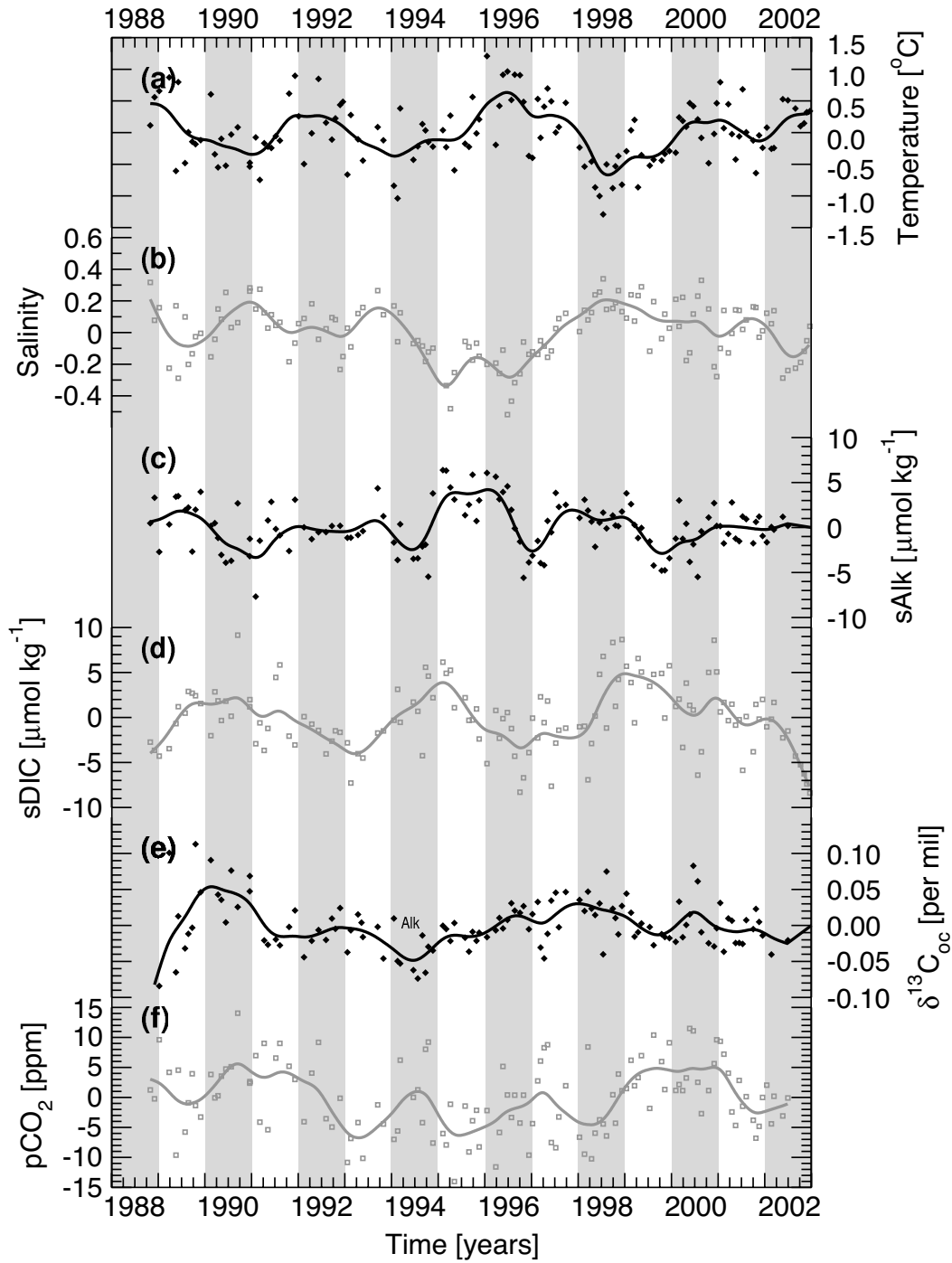


Figure 2. Time-series of anomalies of (a) SST, (b) SSS, (c) sAlk, (d) sDIC, (e) $\delta^{13}\text{C}$, and (f) pCO_2 at Sta. ALOHA. The interannual anomalies have been determined by subtracting linear trends and by removing the average seasonal cycle, computed by fitting harmonic functions with periods of 12, 6, and 4 months to the data. Smoothing spline fits with a cut-off period of about one year have been added (lines) to emphasize the interannual variability component of the anomalies.

Table 1. Correlations between the time-series of interannual anomalies of various observed quantities at Sta. ALOHA. Values in brackets give the likelihood (in %) that correlations are not random; correlations with $p < 0.05$ are in bold face, with $p > 0.05$ in italics). The correlations were computed from 4-monthly averages (DJFM, AMJJ, and ASON).

	SST	SSS	DIC	sDIC	<i>Alk</i> ^a	<i>sAlk</i> ^a	$\delta^{13}\text{C}$	pCO ₂	MLD ^b
SST	1.00	-0.49 (99.8%)	-0.62 (>99.9%)	-0.50 (99.8%)	-0.48 (99.8%)	<i>0.25</i> (87.1%)	<i>0.05</i> (22.5%)	<i>0.16</i> (65.3%)	-0.34 (96.0%)
SSS		1.00	0.94 (>99.9%)	<i>0.04</i> (18.1%)	0.89 (>99.9%)	-0.40 (98.7%)	<i>0.10</i> (45.2%)	<i>0.26</i> (88.9%)	0.36 (97.2%)
DIC			1.00	0.35 (96.8%)	0.89 (>99.9%)	<i>-0.30</i> (93.7%)	<i>0.09</i> (41.4%)	0.35 (97.0%)	0.42 (99.1%)
sDIC				1.00	<i>0.15</i> (61.5%)	<i>0.15</i> (63.2%)	<i>0.06</i> (26.4%)	0.42 (99.1%)	<i>0.27</i> (89.3%)
<i>Alk</i> ^a					1.00	<i>-0.01</i> (5.7%)	<i>0.12</i> (51.9%)	<i>0.10</i> (43.5%)	0.33 (95.5%)
<i>sAlk</i> ^a						1.00	<i>0.01</i> (4.4%)	-0.39 (98.5%)	<i>-0.14</i> (60.5%)
$\delta^{13}\text{C}$							1.00	<i>0.17</i> (70.6%)	<i>0.04</i> (18.6%)
pCO ₂								1.00	<i>0.20</i> (76.4%)
MLD ^b									1.00

^a data from CDRG [Keeling *et al.*, 2004] with seven additional values from the HOT data set [Lukas and Karl, 1999] added in 1994.

^b Estimated from CTD temperatures and salinities [Lukas and Karl, 1999] applying the variable σ_θ criterion of Sprintall and Tomczak [1992] with a temperature difference between the surface and the base of the mixed layer of 0.5°C.

to a short overview.

The model takes advantage of concurrent $\delta^{13}\text{C}$ and DIC data and identifies the following processes influencing these quantities in the surface mixed layer: air-sea gas exchange, vertical diffusion, entrainment, horizontal transport, and net community production (NCP), i.e. the difference between net primary production and heterotrophic respiration [Williams, 1993]. The first three processes are estimated on the basis of observations and simple formulas. Horizontal transport and NCP are diagnosed by the model on the basis of budget constraints that require concurrent observations of DIC and $\delta^{13}\text{C}$.

The model is forced by data which have been separated into three components, a seasonal, a linear trend, and an interannual spline fit, as described in section 2. From these data, a forcing function is constructed consisting of the three annual harmonics and the smoothing spline fit, $S(t)$, but excluding any linear trend of the data, i.e.

$$F(t) = H_0 + \sum_{k=1}^3 \left[a_k \sin\left(\frac{2\pi kt}{T}\right) + b_k \cos\left(\frac{2\pi kt}{T}\right) \right] + S(t), \quad (1)$$

where t denotes a calendar day between 1988 and 2002 and T the length of each calendar year.

For details with regard to the particular choice of input data and parameters for the diagnostic model, the reader is referred to Keeling *et al.* [2004]. The model equations are solved for the period from July 1988 until July 2002. The mean seasonal variability diagnosed by the model is described by Keeling *et al.* [2004]. To address interannual variability, this mean seasonal cycle was subtracted from the fourteen year time-series for all diagnosed quantities.

4. Diagnostic modeling results

Air-sea gas exchange, lateral transport, and NCP exhibit substantial interannual variability with peak-to-peak flux anomalies of up to $\pm 1 \text{ mol m}^{-2} \text{ yr}^{-1}$, whereas flux anomalies for diffusion (not shown) and entrainment are small (Figure 3). A comparison of these flux anomalies with the annual mean carbon fluxes ($0.5 \pm 0.2 \text{ mol m}^{-2} \text{ yr}^{-1}$ for entrainment, $0.5 \pm 0.3 \text{ mol m}^{-2} \text{ yr}^{-1}$ for vertical diffusion, $0.9 \pm 0.8 \text{ mol m}^{-2} \text{ yr}^{-1}$ for lateral transport, $1.0 \pm 0.1 \text{ mol m}^{-2} \text{ yr}^{-1}$ for gas exchange, and $2.3 \pm 0.8 \text{ mol m}^{-2} \text{ yr}^{-1}$ for NCP [Keeling *et al.*, 2004]) reveals that the former three are responsible for modifications of their respective annual mean fluxes by 40–100%.

Interannual variations of air-sea gas exchange, lateral

transport, and NCP tend to persist for several years. This is particularly evident between 1990 and 1992, when anomalies of both gas exchange and lateral transport remain negative for three years, while anomalies of NCP stay positive (Fig. 3). This substantial lower frequency variability is also evident in SST, with similar two to four year periods.

Interannual variability also brings about substantial shifts in the relative contribution of the different processes to upper ocean carbon cycle variations over time. During 1995 to 1996, for example, the uptake of CO_2 from the atmosphere was the dominant process supplying $s\text{DIC}$ to the mixed layer, while lateral transport was unusually weak. However, the additional uptake of CO_2 from the atmosphere was not able to compensate for the smaller lateral supply of $s\text{DIC}$, and since NCP was about average, a distinct negative $s\text{DIC}$ anomaly resulted (see Fig. 2d). In contrast, during 1998 and 1999, lateral transport and air-sea exchange both contributed anomalously large amounts of $s\text{DIC}$ to the mixed layer, while inorganic carbon removal by NCP was again about average, leading to a positive $s\text{DIC}$ anomaly (see Fig. 2d).

In order to better understand the processes underlying these interannual fluctuations, we computed correlations between interannual anomalies of all available quantities. We first highlight correlations of the processes with observations, and then the correlations between the processes themselves.

The strongest correlations between observed quantities and our diagnosed results are found for SST (Table 2). Temperature variability emerges thus as the most important factor influencing the upper ocean carbon cycle at Sta. ALOHA. Air-sea gas exchange ($r = -0.35$) shows the highest correlation with SST, followed by entrainment ($r = +0.34$). The latter correlation is quantitatively not important, as interannual variability of entrainment is small for the upper carbon cycle near Sta. ALOHA (Fig. 3c). Correlations of lateral transport and NCP with SST are small with respect to all seasons (Fig. 3 and Table 2). However, strong seasonal correlations appear when analyzing separately for winter (December–March), spring/summer (April–July), and fall (August–November). In winter, higher temperatures coincide with stronger than normal transport ($r = +0.59$) and higher biological production ($r = -0.55$). In spring/summer, the situation is reversed with positive correlations between SST and NCP ($r = +0.49$). SST and lateral transport are correlated only weakly ($r = -0.07$), then.

Air-sea gas exchange anomalies (Fig. 3b) are anti-

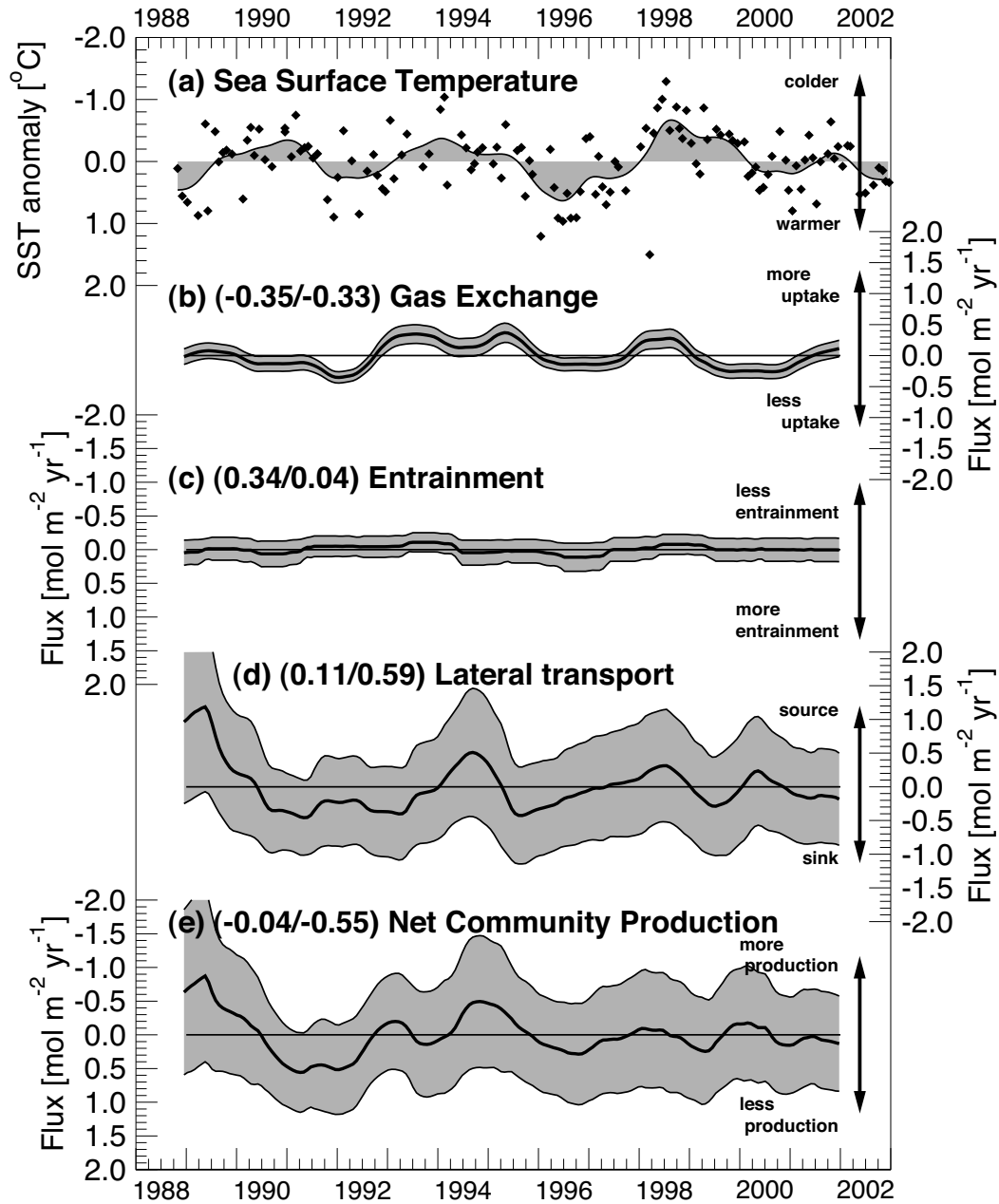


Figure 3. Observed and diagnosed interannual variability at Sta. ALOHA. (a) SST anomalies, with a one year smoothing spline fit (compare Fig. 2a), (b) air-sea gas exchange, (c) entrainment, (d) lateral transport and (e) net community production anomalies. The lines in (b-e) represent \pm one standard deviation uncertainty estimates from Monte Carlo experiments (calculation see Appendix B). Note that the ordinates for (a), (c), and (e) are inverted. Numbers give the correlation between the time-series of SST and the respective process for the entire year (first value) and for DJFM (second value).

Table 2. Correlations between PDO, ENSO, and various observed and diagnosed quantities at Sta. ALOHA. Correlations with $p < 0.05$ are in bold face. See text and Appendix A for data sources.

property ^a	PDO	NINO3.4	WS	SST	sDIC	pCO ₂	Gas. Ex.	Diff.	Ent.	Lat. Trsp.	NCP
PDO	1.00	0.47	-0.36	0.33	-0.42	-0.38	0.29	0.12	-0.06	-0.19	0.14
NINO3.4		1.00	-0.26	0.13	-0.21	-0.12	0.07	-0.05	-0.17	-0.20	0.23
WS			1.00	-0.72	0.39	-0.12	0.38	-0.02	-0.16	0.15	-0.26
SST				1.00	-0.50	0.16	-0.35	-0.05	0.34	0.11	-0.04
sDIC					1.00	0.42	-0.08	-0.11	0.09	0.03	0.07
pCO ₂						1.00	-0.68	-0.13	0.21	0.11	0.23
Gas. Ex.							1.00	0.03	-0.20	0.04	-0.39
Diff.								1.00	-0.13	-0.32	-0.14
Ent.									1.00	0.00	-0.01
Lat. Trsp.										1.00	-0.71
NCP											1.00

^a WS: wind speed; NINO 3.4: ENSO index based on SST anomalies between 5°S and 5°N, and from 170°W to 120°W.

correlated with pCO₂ ($r = -0.68$) and correlated with wind speed ($r = +0.38$). This is a direct consequence of our estimating of air-sea gas exchange as a product of a wind-speed dependent gas exchange coefficient and the air-sea CO₂ partial pressure difference. Air-sea gas exchange and NCP are negatively correlated with an annual correlation coefficient of $r = -0.39$ and an even higher correlation for the spring/summer period ($r = -0.55$). This correlation is likely caused by the NCP induced changes in sDIC, which lead to changes in surface ocean pCO₂ and therefore alter the magnitude of air-sea gas exchange. This explanation is supported by a positive correlation of pCO₂ and NCP during spring/summer ($r = +0.42$).

Net community production and lateral transport are highly anti-correlated throughout the entire time-series ($r = -0.71$). The anomalies of these two quantities at the beginning of the time-series (early 1989) (Fig. 3d and e) need to be viewed cautiously, however, as they are caused by a the steep initial rise and fall of the $\delta^{13}\text{C}$ spline-fit, which could be partly a fitting artifact (Fig. 2e). Sensitivity tests show that this strong correlation between NCP and lateral transport is robust within the uncertainty bounds as shown by our Monte Carlo simulations (see Appendix B) in Figure 3d-e. We therefore do not attribute this correlation to the diagnostic model set up, in which NCP and lateral transport are the two terms for which the DIC and DI^{13}C mass balances are solved for (see *Keeling et al.* [2004] for details).

This anti-correlation between NCP and lateral transport stems from intensified biological production coinciding with increased carbon input by lateral transport. A possible cause of this strong correlation is the transport of nutrients that is associated with the lateral transport of carbon. As biological productivity at

Sta. ALOHA is typically nutrient limited [*Karl et al.*, 1996], enhanced lateral supply of nutrients (especially of dissolved organic phosphorus (DOP), which tends to be higher upstream of the surface flow [*Abell et al.*, 2000]) could lead to intensified NCP. Enhanced DOP could provide the phosphorus necessary to enhance N₂ fixation, which has been shown by *Karl et al.* [1997] and *Dore et al.* [2002] to constitute a substantial fraction of primary production at Sta. ALOHA.

In order to highlight the role of SST variations in controlling interannual variability of the upper ocean carbon cycle near Hawaii, we stratify our findings into years with warm and cold SST anomalies (Figure 4). In warmer than normal years, NCP tends to be reduced by about $0.09 \text{ mol m}^{-2} \text{ yr}^{-1}$, which acting alone would cause increased sDIC, but this tendency is outweighed by weaker uptake of CO₂ from the atmosphere ($-0.18 \text{ mol m}^{-2} \text{ yr}^{-1}$) and a weaker than normal addition of sDIC by lateral transport ($-0.03 \text{ mol m}^{-2} \text{ yr}^{-1}$), which leads to the observed negative sDIC anomalies in warm years. During colder than normal years, the situation tends to be reversed.

We refine this analysis by examining the seasonal dependency of our results (Fig. 5). In winters of warmer than normal years, weakened surface winds and higher oceanic pCO₂ cause a lesser supply of CO₂ to the mixed layer than normal. Reduced input of sDIC by lateral transport and to a lesser degree entrainment strengthen the resulting negative sDIC anomaly, while a reduced NCP compensates somewhat. In spring and summer of warm years, lower than average uptake of CO₂ from the atmosphere continue to cause a negative sDIC anomaly. The impact of this reduced supply is enhanced by a shallower mixed layer, and partially offset by reduced NCP. In winter, spring and summer of cold years, the opposite is the case. In fall, the surface carbon cycle

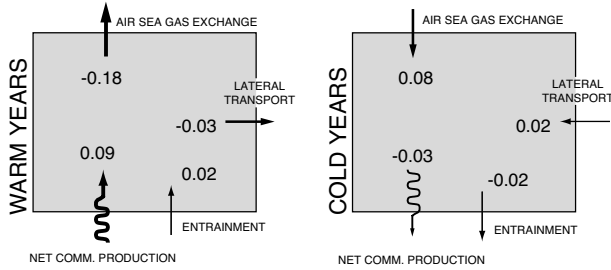


Figure 4. Mean annual flux anomalies for colder than normal years versus those for warmer than normal years. The cold year averages consist of those years, whose annual mean SST anomaly (determined from the spline fit low-passed filtered data) was one half standard deviation below the long-term mean, i.e. 1990, 1993/94, and 1998/99, whereas the warm year averages contain years, whose annual mean SST anomaly was one half standard deviation above the long-term mean, i.e. 1992, 1996/97, and 2000.

at Sta. ALOHA varies little between warmer and colder than normal years, except for lateral transport, which tends to be a slightly stronger source in colder than normal years.

5. Discussion of interannual variability at Sta. ALOHA

5.1. Biological productivity

The availability of various estimates of carbon export permits us to evaluate our diagnosed NCP values with independent estimates. As in *Keeling et al.* [2004], we extrapolate our results from the mixed layer to the euphotic zone by multiplying our mixed layer NCP values by 1.25. Over the annual cycle, NCP can be regarded as being numerically equivalent to export production, i.e. the annual integrated loss of organic carbon from the mixed layer, either in the form of particulate organic carbon (POC), which tends to be exported vertically by sinking, or in the form of dissolved organic carbon (DOC), which can be exported both laterally and vertically.

Fig. 6 shows a time-series of our extrapolated and annually integrated NCP estimates in comparison with various estimates of carbon export. As discussed by *Keeling et al.* [2004], our long-term mean NCP is similar to those reported previously. Since most studies pertain to single years, no direct comparison can be made with regard to interannual variability.

DIC: **negative** anomaly **positive** pCO₂ anomalies
SST: **positive** anomaly in spring/summer

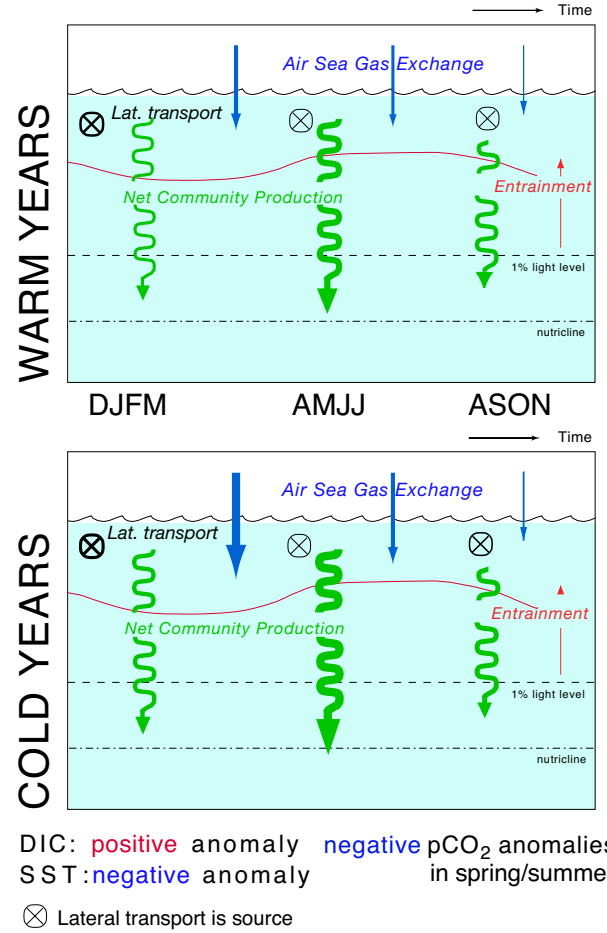


Figure 5. Schematic illustration of the seasonal carbon cycle at Sta. ALOHA and its interannual variability for years with either positive or negative SST anomalies.

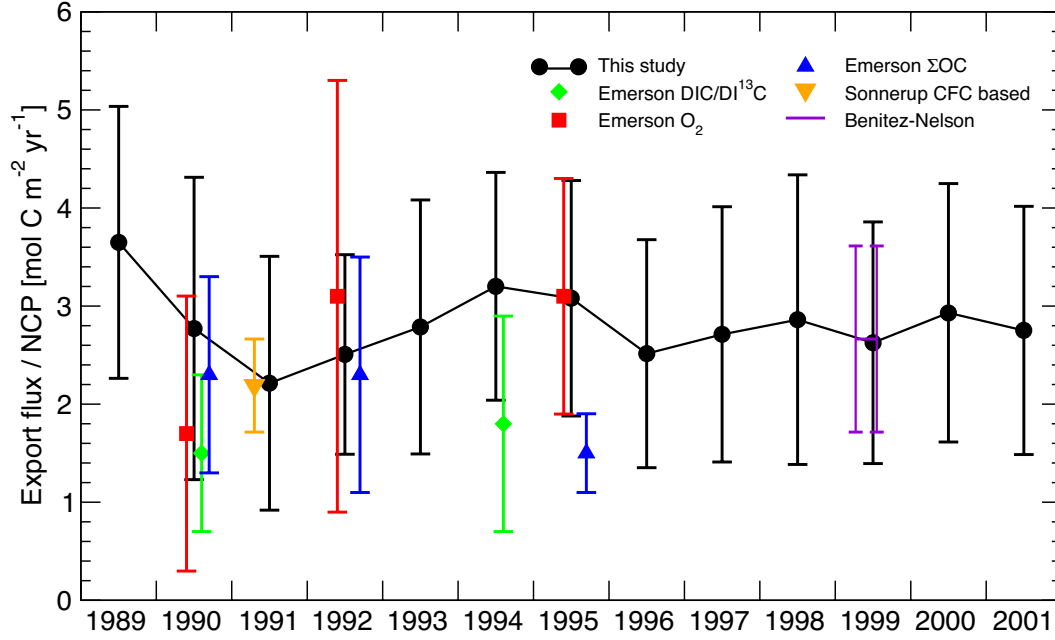


Figure 6. Magnitude of diagnosed annual means for NCP from our model calculations extrapolated to the euphotic zone by multiplying with 1.25 (black dots). The error bars represent uncertainties calculated by Monte-Carlo experiments. As comparisons we show carbon export rates from the upper 100m [Emerson *et al.*, 1997] for measurements of mass balances for inorganic carbon (green diamonds), dissolved oxygen (red squares), and organic carbon (blue triangles). The inverted orange triangle gives a carbon export rate at 150m depth obtained from estimates of oxygen utilization rates based on chlorofluorocarbons [Sonnerup *et al.*, 1999]. The purple line ²³⁴Th based export estimates for the upper 150m [Benitez-Nelson *et al.*, 2001]. For definitions of error bars see the respective publications.

Primary production (PP) was measured by ^{14}C incubation during nearly every occupation of Sta. ALOHA [Karl *et al.*, 1996; Lukas and Karl, 1999], permitting us to investigate the relationship between annually integrated rates of PP and NCP (Figure 7a). If the ratio between export production and PP (termed e-ratio [Laws *et al.*, 2000]) remained constant, all points would have to lie along a single line, whose slope is equal to the e-ratio. Figure 7a shows that about half of the points indeed lie close to a line with a slope of 0.2, suggesting that NCP and PP generally track each other well. There are, however, a number of years that fall considerably away from this line of constant e-ratio. The most notable exceptions are 1991 with an e-ratio of 0.14, 2000 with an e-ratio of 0.15, and 1990 and 1994 with e-ratios of 0.26. The anomalously low e-ratio in 1991 is mainly driven by lower than average NCP, the low e-ratio in 2000 is caused by high PP. The anomalously high e-ratio in 1990 is due to lower than normal PP while 1994 both relatively high NCP and lower than normal PP cause the high e-ratio.

The empirical relationship of Laws *et al.* [2000] predicts lower e-ratios during warm years and higher e-ratios during cold years. However, these four years do not stand out as being particularly cold or warm (see Figure 2a). Therefore other reasons must be responsible for these anomalies in the e-ratio.

The most important process that could cause a decoupling between PP and NCP is a change in ecosystem structure, as this alters the efficiency with which organic matter produced within the euphotic zone is remineralized and respired. For example, one would expect that an ecosystem shift, in which a higher fraction of freshly produced organic matter ends up as DOC rather than POC, would lead to a higher recycling efficiency, i.e. lower e-ratio.

If this were the case, one would expect a relatively good correspondence between the fraction of PP that is exported as POC (pe-ratio, [Dunne *et al.*, 2004]) and the e-ratio. The ratio of these quantities is equal to the fraction of export that occurs in form of POC, which we term p-ratio. As Figure 7b shows, the relationship between POC export and NCP is rather variable, with the early 1990s having high p-ratios, the years from 1992 to 1995 being characterized by low p-ratios, and the years from 1996 to 2000 having intermediate p-ratios of about 0.29 to 0.36. Thus 29% to 36% of export production is exported vertically in the form of sinking POC. Therefore, variations in the fraction of PP that goes into particulate organic matter export do not appear to be the cause of the variations in the e-ratio. Given the

lack of any other characteristic anomaly that describes the years 1990, 1991, 1994, and 2000 (see Figure 2) the cause for the e-ratio variations remain unclear.

The observation that the relationship between export in the form of POC and NCP fall into three modes merits further discussion. A similar grouping was observed by Dore *et al.* [2002] when they investigated the particulate organic nitrogen (PON) export variations at Sta. ALOHA. Using measurements of the $\delta^{15}\text{N}$ ratio of PON, they determined the relative contribution of N_2 fixation to PON export. Based on these data, they suggested that times of record before 1991 can be characterized as an “energetic period”, during which most of the nitrogen was supplied to the upper ocean ecosystem as nitrate. They postulated that the period from 1992 to 1995 was one of persistent stratification, with low fluxes of nitrate and low contributions from N_2 fixation. They described 1996 to 2000, as a “moderate period”, in which the supply of nitrate is relatively low, but conditions for N_2 fixation are favorable, leading to a relatively high relative contribution of N_2 fixation to PON export.

Mapping these three periods onto 7b shows that during the period of persistent stratification, i.e. 1992–1995, the smallest fraction of export (25% and less) occurs in the form of vertically sinking particles. The remaining fraction of export must be exported as DOC or through other means, such as vertically migrating zooplankton [Steinberg *et al.*, 2000]. In contrast, during the “energetic period”, i.e. the early 1990s, almost 40% of export occurs in the form of sinking particles. The “moderate period” is characterized by intermediate values of 30% to 35%. The ecosystem changes that give raise to these changes in the relative export of POC, presumably versus DOC, are not clear, except that the $\delta^{15}\text{N}$ data suggest that it is not directly related to the fraction of PON export that is fueled by N_2 fixation.

5.2. Air-sea CO_2 fluxes

Air-sea CO_2 flux variability in the North Pacific has been simulated by two global three-dimensional coupled physical-biogeochemical models that were forced with observed variations in winds, and air-sea fluxes of heat and freshwater [Le Quéré *et al.*, 2000; McKinley *et al.*, 2004]. The modeled air-sea CO_2 flux anomalies for the grid-box that contains Sta. ALOHA are compared to our observationally based flux anomalies in Figure 8. In general, the model simulated interannual variability is similar in amplitude to the observed air-sea CO_2 flux variability, but there exist substantial phase differences between the two models, as well as between the models

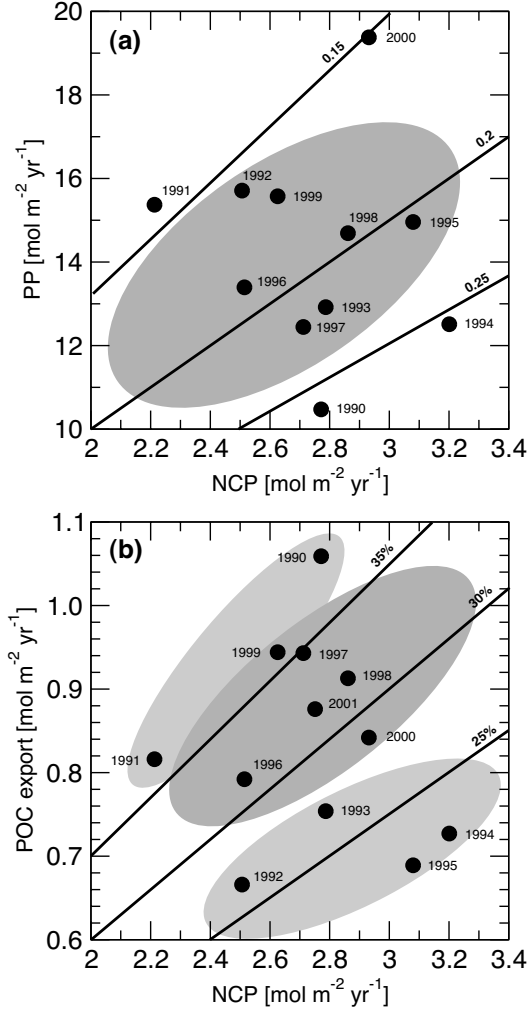


Figure 7. Annual mean values of diagnosed net community production (NCP) versus (a) primary production (PP), and (b) particulate organic matter (POM) export at Sta. ALOHA [Lukas and Karl, 1999]. The diagonal lines give (a) constant e-ratios and (b) constant p-ratios, i.e. constant fractions of export as particles. Ellipses highlight years having similar e- or p-ratios.

and observationally based estimates. A comparison of SST anomalies between the models and the in-situ observations does not exhibit significant differences, nor should the respective wind-speeds employed in these studies be substantially different, as they are all directly based on observations. Therefore, it appears that the models have some difficulty in correctly modeling the temporal evolution of the mixed layer DIC variations, perhaps because of misrepresentations of variations in biological productivity and/or lateral transport.

6. Interannual variability in the subtropical gyres

Interannual anomalies of meteorological forcing at an open ocean site such as Sta. ALOHA occur synchronously over large areas, which may, for instance, extend over a substantial fraction of the subtropical gyre of the North Pacific. We therefore are interested in establishing potential links between our local observations and large-scale phenomena that can reveal the relevance of our results for the subtropical gyres as a whole.

6.1. Connections to large-scale climate patterns

The El Niño-Southern Oscillation and the Pacific Decadal Oscillation are the two known dominant climate modes in the North Pacific. With regard to ENSO, only weak correlations with SST anomalies near Hawaii could be established. The only meteorological forcings near Hawaii that exhibit notable correlations with ENSO are winds and precipitation, both of which tend to decrease near Hawaii during El Niño years [Rasmusson and Carpenter, 1982]. Whether and how these different meteorological forcings impact the upper ocean carbon cycle near Hawaii and might lead to correlations of upper ocean carbon cycle parameters with ENSO has not been determined yet. Karl *et al.* [1995] and Karl *et al.* [1996] argued that such a connection might indeed exist, as they found that the increased stratification and changed circulation pattern during the 1990–1992 prolonged ENSO event coincided with a nearly 3-year sustained increase in primary production (PP). However, their time-series was too short to substantiate this conclusion statistically.

Precipitation around Hawaii appears to be the factor most strongly connected to PDO, with drier conditions prevailing during negative phases of the PDO. Such changes in precipitation could impact the upper ocean carbon cycle mainly through changes in surface alkalinity, which alters the ability of the surface ocean

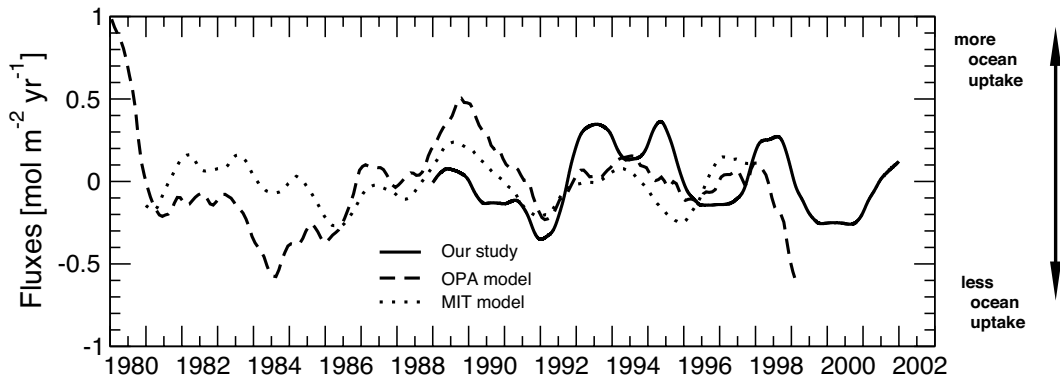


Figure 8. Comparison of anomalous air-sea gas exchange flux estimates for Sta. ALOHA. Shown are our estimates based on observed winds and calculated oceanic $p\text{CO}_2$, and also the model derived estimates from *Le Quéré et al.* [2000] (OPA model) and *McKinley et al.* [2004] (MIT model).

to contain DIC [*Dore et al.*, 2003; *Keeling et al.*, 2004]. *Keeling et al.* [2004] suggested that such a change occurred in the late 1990s around Sta. ALOHA, when a phase change of the PDO drove a substantial increase in surface ocean alkalinity by increasing salinity, which then caused an increase in surface ocean DIC. However, more generally, the impact of PDO on interannual variability in the upper ocean carbon cycle has not been established.

It is therefore of particular interest to investigate possible links between these two climate modes and the observed variability at Sta. ALOHA. Figure 9 shows the temporal evolution of the indices of these two climate patterns (see Appendix A for sources) in comparison to our diagnosed flux anomalies at Sta. ALOHA. As evidenced in this figure, and more particularly in Table 2, the correlations of our diagnosed flux anomalies with either PDO or ENSO are generally only small to moderate.

For ENSO, none of our calculated quantities shows a correlation that is statistically significant at the 95% confidence level. For NCP and NINO3.4 (see Appendix A for reference) we determine a correlation value of $r=+0.23$. A correlation of more than $r=+0.35$ found for a 10 to 14 months lag (NINO3.4 leading) is similar to the 10 months lag correlation identified by *Dore et al.* [2002] between ENSO and PON export. These positive correlations indicate that NCP is reduced during and slightly after positive phases of ENSO. Diminished horizontal transport of DIC, and perhaps of nutrients, to the area near Sta. ALOHA is also indicated, possibly explaining the lower productivity.

A positive correlation between ENSO and NCP over

our record period is evident from 1988 until 1991, while ENSO was going from a La Niña phase into a nearly four year persistent state of weak to moderate El Niños. This correlation supports the findings of *Karl et al.* [1995], who hypothesized that the stratification of the upper ocean during this period was increased, reducing the input of new nitrate, enhancing N_2 fixation, and reducing export. However, the impact of ENSO on biological productivity at Sta. ALOHA appears intermittent. There is no indication for changes near Hawaii associated with the 1997/1998 El Niño, which was one of the strongest of the 20th century [*McPhaden*, 1999].

Correlations of upper ocean carbon cycle variability near Hawaii with the PDO index are generally higher than those for ENSO. In addition to warmer SSTs, years with positive PDO index tend to be associated with lower wind speeds ($r=-0.36$) (Table 2). These correlations can be explained by the weakening of the Aleutian low during positive phases of the PDO and the associated weakening of the high pressure system over the subtropics (see e.g. *Miller and Schneider* [2000]). The resulting reduction in the surface pressure gradient leads to a slackening of the winds over the North Pacific, including Hawaii. These calmer than normal weather conditions are associated with negative $p\text{CO}_2$ anomalies ($r=-0.38$), but the effect on air-sea gas exchange is reduced, as the weaker winds tend to counteract the effect of negative oceanic $p\text{CO}_2$ anomalies, yielding a correlation between PDO and gas exchange of only $r=+0.29$. The lower than normal oceanic $p\text{CO}_2$ during positive phases of the PDO are mainly a result of negative $s\text{DIC}$ anomalies ($r=-0.42$), which themselves are caused by weaker than normal entrainment, lateral

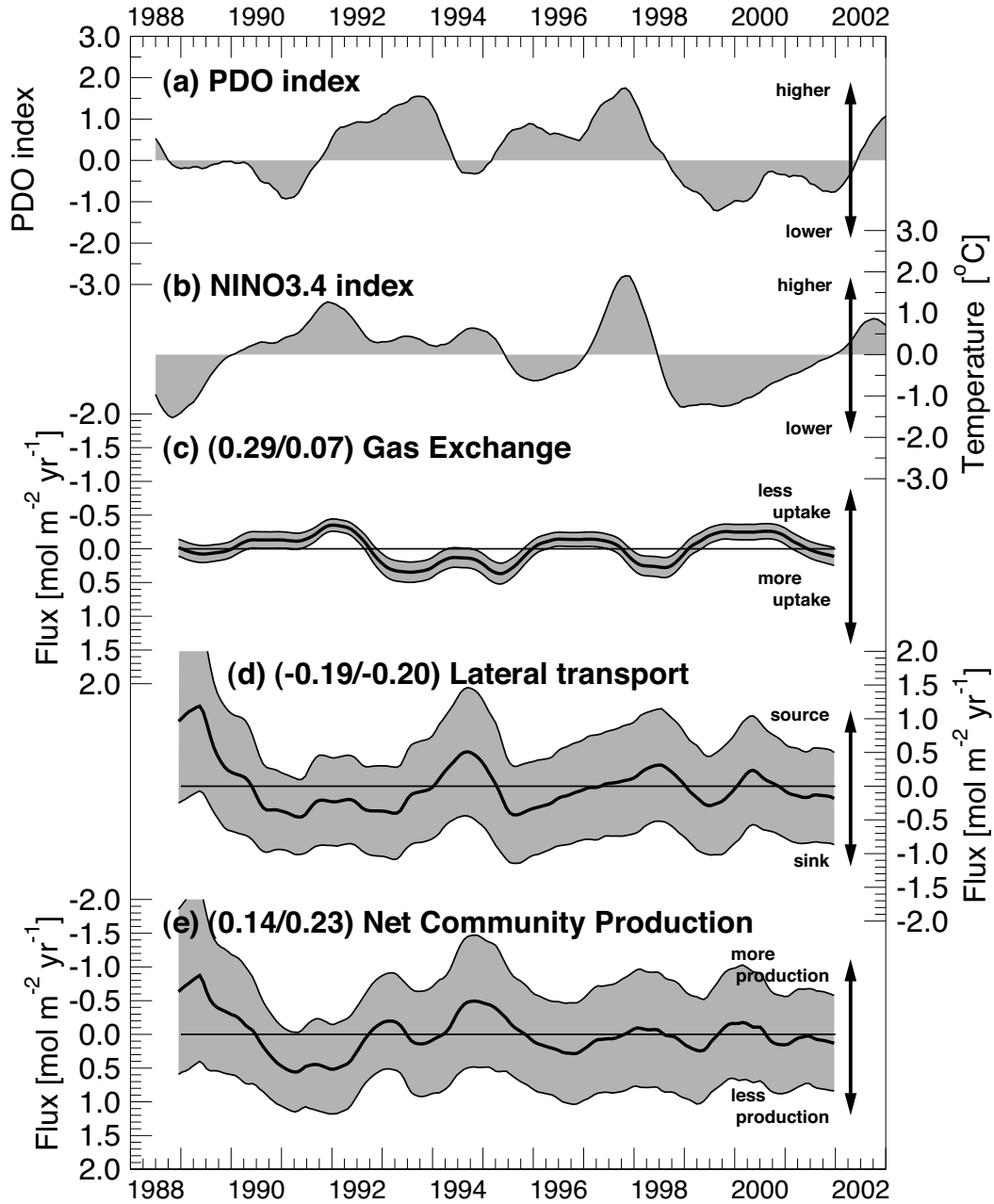


Figure 9. Comparison of interannual variability of carbon fluxes at Sta. ALOHA with indices of the El Niño-Southern Oscillation and the Pacific Decadal Oscillation. The values in brackets denote the correlation coefficient for the PDO and ENSO, respectively. Flux anomalies for gas exchange, lateral transport and net community production are from Figure 3. See Appendix A for sources of ENSO and PDO indices.

transport and reduced NCP. Neither of these correlations are statistically significant, however.

Why are the correlations of variations of the upper ocean carbon cycle near Hawaii with ENSO so small and why are they somewhat larger for PDO? Figure 10, which shows the correlations of SST anomalies in the Pacific with ENSO, PDO, and SST anomalies near Hawaii, provides preliminary answers. While SST anomalies at Sta. ALOHA are highly correlated or anti-correlated with SST anomalies over a substantial fraction of the North Pacific (Fig. 10 a, see also *McGowan [1995]*), the correlations with the tropical Pacific are small. The pattern of correlation of SST anomalies in the Pacific with ENSO (Fig. 10 c) reveals that this is because Hawaii sits on the ridge (in SST) between a region of strongly positively correlated SST anomalies in the eastern and central tropical Pacific, and negatively correlated SST anomalies in the north-western subtropical and temperate North Pacific. This situation leads to a very small correlation between SST anomalies at Sta. ALOHA and the NINO3.4 index ($r=+0.13$, Table 2). In contrast, the pattern of correlation between SST anomalies in the North Pacific and those observed near Hawaii shows some similarity with the subtropical and subpolar part of the PDO regression pattern (Fig. 10 b), leading to a higher correlation coefficient between SST anomalies at Sta. ALOHA and the PDO index ($r=+0.33$, Table 2).

A second reason for relatively low correlations between ENSO, PDO, and variations near Hawaii is that these two modes together explain only about 30% of the variance observed in various quantities in the North Pacific. (Principal component analyses give values of 27% for 31 climate time series in the North Pacific for PDO related variability [*Hare and Mantua, 2000*], and 19% for ENSO related variability.) This means that most of the variance in climate variability in the North Pacific is unrelated to either PDO or ENSO.

While correlations between variations at Sta. ALOHA with ENSO and PDO on interannual time-scales are relatively small, the impact of longer time-scale variations in these two climate modes may lead to a larger imprint. *Keeling et al. [2004]* suggested, for example, that the marked increase in SSS and $sDIC$ at Sta. ALOHA in 1996/1997 (Figures 1 and 2) and the suppression of the CO_2 sink at Sta. ALOHA from 1996 to 2001 may be connected to a large scale climate regime shift in the late 1990s, which is possibly related to the PDO [*Mantua and Hare, 2002; Chavez et al., 2003; Peterson and Schwing, 2003*].

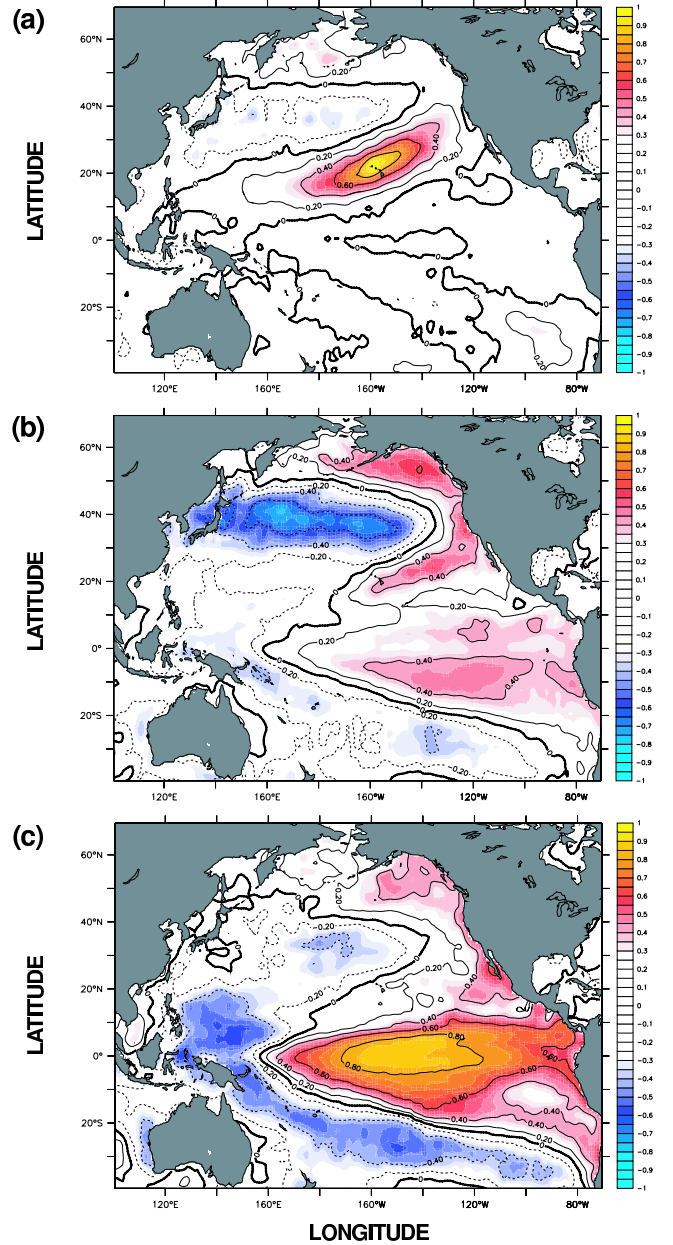


Figure 10. Spatial patterns of the correlation of the Reynold’s Optimum Interpolation SST data for November 1988 through December 2001. (a) Correlation with SST at Sta. ALOHA, (b) correlation with the PDO index, and (c) correlation with the NINO3.4 index of ENSO. For data sources see text and Appendix A.

6.2. Air-sea CO₂ flux variability in the NPSG

The basin-wide scale of SST correlations in Figure 10 suggests that the observed interannual variability in the upper ocean carbon cycle at Sta. ALOHA might be representative of variability at least for the southern part of the North Pacific Subtropical Gyre (NPSG). We investigate the implications of this hypothesis by estimating the magnitude of interannual variability of air-sea fluxes for the area between 10°N and 30°N using two extrapolation methods.

In the first method, assuming that the entire southern NPSG varies in concert with Hawaii, we multiply the gas exchange anomalies with the area (defined here as the region between 10°N and 30°N, and 100°W and 100°E, i.e. $35.4 \times 10^{12} \text{m}^2$), and obtain gas exchange anomalies of $\pm 0.25 \text{ Pg C yr}^{-1}$. In our second approach, relying on SST as our master variable, we use observed SST anomalies and an empirically derived temperature sensitivity of the gas exchange flux from Sta. ALOHA to extrapolate our results to the southern NPSG. Fitting a linear function by least squares to a plot of our gas exchange flux anomalies, $F_{\text{gas ex}}$, versus SST anomalies yields a slope of $\partial F_{\text{gas ex}} / \partial T = -0.36 \pm 0.30 \text{ mol m}^{-2} \text{ yr}^{-1} (\text{°C})^{-1}$. This compares to a slope of $-0.57 \pm 0.01 \text{ mol m}^{-2} \text{ yr}^{-1} (\text{°C})^{-1}$ for the seasonal cycle, i.e. a value within the bounds of the analysis of the interannual anomalies. Multiplying the interannual slope with the observed SST anomaly fields yields gas exchange anomalies for the entire southern NPSG of $\pm 0.08 \text{ Pg C yr}^{-1}$.

The climatological annual net uptake of CO₂ for the same area is about 0.1 Pg C yr^{-1} [Takahashi *et al.*, 2002]. Thus, interannual variability of air-sea CO₂ exchange in the southern NPSG is likely to amount to more than 50% of the mean uptake. The two biogeochemical ocean models, whose air-sea flux variability at Sta. ALOHA is shown in Figure 8, simulate air-sea CO₂ flux variability for the same area of $\pm 0.12 \text{ Pg C yr}^{-1}$ [Le Quéré *et al.*, 2000] and $\pm 0.07 \text{ Pg C yr}^{-1}$ [McKinley *et al.*, 2004], similar to our second SST derived estimate.

6.3. Comparing subtropical gyres: HOT versus BATS

Analyses similar to those presented in this study have also been performed for the subtropical gyre of the North Atlantic using carbon data from the Bermuda Atlantic Time-Series (BATS) site and from Hydrostation "S" [Bates, 2001; Gruber *et al.*, 2002]. BATS and Station "S" in combination and Sta. ALOHA share several similarities, but due to the more southerly and cen-

tral location within the Pacific subtropical gyre, the seasonal cycle of heating/cooling is much smaller at Sta. ALOHA, resulting in a reduced annual cycle of SST and much smaller seasonal changes in mixed layer depth. It is instructive to compare the magnitudes and mechanisms of upper ocean variability in the carbon cycle between the two sites.

The ranges of interannual variability (measured peak-to-peak) are about the same at both sites (e.g. 1° to 1.5°C for SST, approx. $10 \mu\text{mol kg}^{-1}$ for $s\text{DIC}$, and 0.1‰ for $\delta^{13}\text{C}$) with slightly higher values at BATS. This contrasts to the seasonal amplitudes which are twice as large at BATS (8°C vs. 4°C ; $30\text{--}40 \mu\text{mol kg}^{-1}$ vs. $15\text{--}20 \mu\text{mol kg}^{-1}$; and 0.2‰ 0.1‰) [Gruber *et al.*, 1998; Keeling *et al.*, 2004]. Similar to findings at Sta. ALOHA, Bates [2001] and Gruber *et al.* [2002] found an anti-correlation between interannual anomalies of SST and $s\text{DIC}$ at BATS, but with a correlation coefficient that is higher than that at Sta. ALOHA. At both sites, these anti-correlations lead to a suppression of the correlation of both quantities with surface ocean pCO₂. On interannual time-scales, the forcing of temperature on pCO₂ appears to be dominating over the forcing by $s\text{DIC}$ at BATS, while $s\text{DIC}$ forcing tends to dominate at Sta. ALOHA. Salinity and Alk are correlated at the North Atlantic station with a slightly weaker coefficient (0.69 against 0.89 at the HOT site), while SSS and $sAlk$ show the nearly the same anti-correlation at both sites. At BATS, $\delta^{13}\text{C}$ is well correlated with SST, $s\text{DIC}$, and with mixed layer depth [Gruber *et al.*, 2002]. In contrast, $\delta^{13}\text{C}$ shows negligible correlations with all other quantities at Sta. ALOHA.

Both sites show substantial interannual variability in estimated gas exchange and NCP, which constitute two of the three processes that dominate the carbon balance on interannual as well as on seasonal time scales. The third dominant interannual contribution is entrainment near Bermuda but lateral transport near Hawaii. The range of the variabilities of these processes is similar at both sites, with a tendency for higher values at BATS. Air-sea gas exchange at both sites varies in concert with SST and wind speed anomalies (near Hawaii mainly during spring and summer). Variations in NCP and entrainment near Bermuda are significantly correlated with variations in mixed layer depths, probably due to the associated changes in the entrainment of new nutrients into the upper ocean. In contrast, due to the absence of large variations in winter mixed layer depths, variations in NCP near Hawaii are only weakly connected to vertical nutrient supplies. The high correlation of variations in NCP and lateral transport suggests,

however, that this latter process is important in supplying additional nutrients to the area north of Hawaii. In summary, interannual variations of mixed layer depth emerge as the main factor controlling interannual variability at BATS, while variations of SST and lateral transport are the main processes at Sta. ALOHA.

The two stations differ with regard to the relation of their interannual to decadal variability to large-scale climate modes. On interannual time-scales, the link between variability near Sta. ALOHA and ENSO is intermittent and weak, while this link is slightly stronger to PDO. A stronger link to PDO on decadal time-scales may exist, but the data record is too short to substantiate this hypothesis. At BATS, the North Atlantic Oscillation (NAO) exerts a substantial influence on winter convection and SSTs. This leads to interannual variabilities of NCP and air-sea gas exchange fluxes that are statistically well correlated with NAO [Gruber *et al.*, 2002]. In years with negative NAO index (i.e. a smaller-than-normal latitudinal pressure gradient in the North Atlantic) air-sea fluxes tend to be intensified and NCP enhanced. Further changes associated with NAO have been identified in the rate of DIC accumulation in mode waters at BATS [Bates *et al.*, 2002].

Let us now extrapolate the observed interannual air-sea CO₂ flux variability at BATS to the North Atlantic subtropical gyre in a manner similar to that done above for the subtropical North Pacific. A correlation analysis of SST anomalies at BATS with those for the entire North Atlantic shows that interannual variability at BATS can be viewed as being representative for the North Atlantic subtropical gyre between 25°N and 45°N ($15.3 \times 10^{12} \text{m}^2$). A direct multiplication of the gas exchange fluxes at BATS with this surface area yields an interannual variability of air-sea CO₂ fluxes of approximately $\pm 0.15 \text{ Pg C yr}^{-1}$. The slope of the relationship between gas exchange and SST is somewhat higher near BATS, with a value of $\partial F_{\text{gas ex}} / \partial T = -0.98 \pm 0.30 \text{ mol m}^{-2} \text{ yr}^{-1} (^\circ\text{C})^{-1}$. Multiplying this slope with the observed SST anomalies leads to a air-sea CO₂ flux variability of $\pm 0.18 \text{ Pg C yr}^{-1}$. As the climatological mean CO₂ uptake for this area of the North Atlantic is 0.2 Pg C yr^{-1} [Takahashi *et al.*, 2002], it appears possible that interannual variability might lead to $\pm 100\%$ changes in this flux.

Air-sea CO₂ flux variability estimated by the two biogeochemical models for the same area is substantially smaller than our extrapolations. The OPA model of Le Quéré *et al.* [2000] estimates an air-sea CO₂ flux variability of $\pm 0.04 \text{ Pg C yr}^{-1}$ and the MIT model of McKinley *et al.* [2004] a variability of $\pm 0.07 \text{ Pg C}$

yr^{-1} . Possible reason for this discrepancy might be our choice of the gyre area. Takahashi *et al.* [2002] pointed out that the seasonal cycle of pCO₂ changes from being controlled by SST south of 40°N to being controlled by surface ocean DIC north of 40°N. This change may also apply to interannual variations. Although it is not clear whether the models are able to capture these processes correctly, this change of the controlling variable definitely would limit the validity of our extrapolation.

6.4. Subtropical gyres and atmospheric CO₂

We return finally to our initial question about the role of the subtropical gyres in modulating atmospheric CO₂ on interannual time-scales. Our extrapolations suggest that the air-sea CO₂ fluxes in the subtropical gyres of both the North Atlantic and the North Pacific are modulated substantially about their climatological means. Our estimated variability (between ± 0.1 and $\pm 0.2 \text{ Pg C yr}^{-1}$ for both extrapolations) refers to roughly half the area of the respective subtropical gyres. We cannot, however, assume that entire gyres, or even larger ocean regions, act in phase, and we therefore cannot simply add up the above peak-to-peak variations. However, given the observation that high-latitude climate variability tends to be larger than that at mid-latitudes, and that the tropical Pacific is known to vary by up to $\pm 0.4 \text{ Pg C yr}^{-1}$ [Feely *et al.*, 1999; Chavez *et al.*, 1999] there exists the possibility that the ocean contributes substantially to the observed interannual variability of atmospheric CO₂. A reliable quantification, though is beyond the scope of this study.

7. Summary and conclusions

We examined interannual variability of the upper ocean carbon cycle in the North Pacific Subtropical Gyre on the basis of a 14-year time-series of carbon parameters measured at Sta. ALOHA, the site of the HOT program. Our analysis is aided by concurrent measurements of DIC and of its ¹³C/¹²C isotopic ratio which permits us, together with a suite of additional observations, to deduce quantitatively the contribution of the various processes that control interannual variability at this site.

This diagnostic analysis reveals that interannual variability in the oceanic carbon cycle at Sta. ALOHA is a result of an interplay of air-sea gas exchange, net community production, and lateral transport, with sea surface temperature and lateral transport being the key external driving factors. The upper ocean carbon cycle tends to be weakened in warmer and intensified in colder

than average years. Reduced lateral transport and diminished uptake of CO_2 from the atmosphere result in lower DIC concentrations in warmer than average years, despite a partial compensation by weakened NCP.

The influence of ENSO on the upper ocean carbon cycle is detectable during distinct El Niño events, yet overall correlations of ENSO with the investigated quantities are small and for the most part statistically not significant. The Pacific Decadal Oscillation appears to be reflected more strongly in observations at Sta. ALOHA, but also explains only less than 20% of the observed variance.

Interannual variability of the upper ocean carbon cycle at Sta. ALOHA is found to be of similar magnitude to that observed at the BATS site in the subtropical North Atlantic, although the variability there is more strongly governed by mixed layer depth variations. Under the assumption that both stations are representative for large parts of their respective gyres, we postulate that interannual variability in air-sea CO_2 fluxes in these regions is substantial. The observation of a substantial response of the ocean carbon cycle to changes in meteorological forcing suggests that the ocean carbon cycle may respond quite sensitively to future climate change, possibly giving rise to positive feedbacks in the earth system [Sarmiento *et al.*, 1998; Plattner *et al.*, 2001; Gruber *et al.*, 2004].

Acknowledgments.

We are grateful to the numerous people that were involved in the collection, preparation and analysis of the data presented here. Without their dedication, careful work and enthusiasm, this study would not have been possible. We would like to thank in particular Peter Guenther, Tim Lueker, Guy Emanuele, Elaine Bollenbacher, and Andrew Dickson at the Scripps Institution of Oceanography. We are grateful to Dave Karl, Chris Winn, John Dore, Chris Sabine, and many others for their help in collecting water samples and supporting our efforts. We also would like to thank Nathan Mantua for providing the PDO data and figures and Corinne Le Quéré and Galen McKinley for sharing the results of their model runs. We would also like to thank an anonymous reviewer for valuable and constructive comments that helped improve the manuscript. NG and HB acknowledge support from the U.S. National Science Foundation (OCE-0097337); CDK from OCE-0083918 and ATM-0120527.

Appendix A: Data Sources

For Pacific-wide variations in SST, we use Reynold's optimum interpolation (OI) data provided by the NOAA-CIRES Climate Diagnostics Center, Boulder, Colorado, USA, from

their web site at <http://www.cdc.noaa.gov/>. As an index for the Pacific Decadal Oscillation, we adopt that of Mantua *et al.* [1997], which is based on the first principal component of an empirical orthogonal function analysis of monthly SST anomaly fields in the North Pacific. Values of this index were supplied by N. Mantua (pers. comm., 2003). We use the NINO3.4 index to describe the temporal evolution of El Niño-Southern Oscillation. This index is based on the monthly SST anomaly in the region 5°N to 5°S and 170°W to 120°W . Its values were obtained from the U.S. National Oceanic and Atmospheric Administration's Climate Prediction Center through their website: <http://www.cpc.ncep.noaa.gov/data/indices/>.

Appendix B: Uncertainties

Measurement techniques for the data set used in this study have been described in detail in Appendix A of Keeling *et al.* [2004], where accuracy and precision associated with these measurements are listed. Unless stated otherwise the uncertainties ascribed to observational data in the text of this study refer to plus/minus one standard deviation.

To address uncertainties in the model parameters, Monte Carlo experiments [Rubinstein, 1981] were performed (see Gruber *et al.* [1998] for details), in which a random set of values were chosen from a predefined parameter set (shown in Table C4 in Keeling *et al.* [2004]) for each simulation. From the results of these runs, a standard deviation was computed for each term and for each time-step of the model.

Sensitivity studies regarding the number of harmonics used for $\delta^{13}\text{C}$ and variations in the horizontal DIC gradient showed that the modeling results are quite robust. Using only two harmonics for $\delta^{13}\text{C}$ for instance led to variations of less than 5% for NCP and lateral transport fluxes.

References

- Abell, J., S. Emerson, and P. Renaud (2000), Distributions of TOP, TON, and TOC in the North Pacific subtropical gyre: Implications for nutrient supply in the surface ocean and remineralization in the upper thermocline, *J. Mar. Res.*, *58*(2), 203–222.
- Bacastow, R. B. (1976), Modulation of atmospheric carbon dioxide by the Southern Oscillation, *Nature*, *261*, 116–118.
- Baker, D. F. (2001), Sources and sinks of atmospheric CO₂ estimated from batch least-squares inversions of CO₂ concentration measurements, Ph.D. thesis, Princeton Univ., Princeton, NJ, 414 leaves (2 vols.).
- Bates, N. R. (2001), Interannual variability of oceanic CO₂ and biogeochemical properties in the western North Atlantic subtropical gyre, *Deep-Sea Res. II*, *48*(8-9), 1507–1528.
- Bates, N. R., A. F. Michaels, and A. H. Knap (1996), Seasonal and interannual variability of oceanic carbon dioxide species at the U.S. JGOFS Bermuda Atlantic Time-series Study (BATS) site, *Deep-Sea Res. II*, *43*(2-3), 347–383.
- Bates, N. R., A. C. Pequignat, R. J. Johnson, and N. Gruber (2002), A short-term sink for atmospheric CO₂ in Subtropical Mode Water of the North Atlantic Ocean, *Nature*, *420*, 489–493.
- Benitez-Nelson, C., K. O. Buesseler, D. M. Karl, and J. Andrews (2001), A time-series study of particulate matter export in the North Pacific Subtropical Gyre based on ²³⁴Th:²³⁸U disequilibrium, *Deep-Sea Res. I*, *48*(12), 2595–2611.
- Bjerknes, J. (1969), Atmospheric teleconnections in the tropical Pacific, *Mon. Wea. Rev.*, *97*, 103–172.
- Bousquet, P., P. Peylin, P. Ciais, C. Le Quéré, P. Friedlingstein, and P. P. Tans (2000), Regional changes in carbon dioxide fluxes of land and oceans since 1980, *Science*, *290*, 1342–1346.
- Chavez, F. P., P. G. Strutton, G. E. Friederich, R. A. Feely, G. C. Feldman, D. G. Foley, and M. J. McPhaden (1999), Biological and chemical response of the equatorial Pacific Ocean to the 1997–98 El Niño, *Science*, *286*, 2126–2131.
- Chavez, F. P., J. Ryan, S. E. Lluch-Cota, and M. Niquen C. (2003), From anchovies to sardines and back: Multi-decadal change in the Pacific Ocean, *Science*, *299*, 217–221.
- Conway, T. J., P. P. Tans, L. S. Waterman, K. W. Thoning, D. R. Kitzis, K. A. Masarie, and N. Zhang (1994), Evidence for interannual variability of the carbon cycle from the National Oceanic and Atmospheric Administration/Climate Monitoring and Diagnostics Laboratory global air sampling network, *J. Geophys. Res.*, *99*(D11), 22,831–22,855.
- Cramer, W., et al. (2001), Global response of terrestrial ecosystem structure and function to CO₂ and climate change: Results from six dynamic global vegetation models, *Global Change Biology*, *7*(4), 357–373.
- Dore, J. E., J. R. Brum, L. M. Tupas, and D. M. Karl (2002), Seasonal and interannual variability in sources of nitrogen supporting export in the oligotrophic subtropical North Pacific Ocean, *Limnol. Oceanogr.*, *47*(6), 1595–1607.
- Dore, J. E., R. Lukas, D. W. Sadler, and D. M. Karl (2003), Climate-driven changes to the atmospheric CO₂ sink in the subtropical North Pacific Ocean, *Nature*, *424*, 754–757, doi:10.1038/nature01885.
- Dunne, J. P., R. A. Armstrong, A. Gnanadesikan, J. L. Sarmiento, and R. D. Slater (2004), Empirical and mechanistic models for particle export ratio, *Global Biogeochem. Cycles*, submitted.
- Emerson, S., P. Quay, D. Karl, C. Winn, and L. Tupas (1997), Experimental determination of the organic carbon flux from open-ocean surface waters, *Nature*, *389*, 951–954.
- Enting, I. G. (1987), On the use of smoothing splines to filter CO₂ data, *J. Geophys. Res.*, *92*(D9), 10,977–10,984.
- Feely, R. A., R. Wanninkhof, T. Takahashi, and P. Tans (1999), Influence of El Niño on the equatorial Pacific contribution to atmospheric CO₂ accumulation, *Nature*, *398*(6728), 597–601.
- Francey, R. J., P. P. Tans, C. E. Allison, I. G. Enting, J. W. C. White, and T. M. (1995), Changes in oceanic and terrestrial carbon uptake since 1982, *Nature*, *373*, 326–330.
- Gruber, N., and C. D. Keeling (1999), Seasonal carbon cycling in the Sargasso Sea near Bermuda, *Scripps Institution of Oceanography, Bulletin*, *30*, 96.
- Gruber, N., C. Keeling, and T. Stocker (1998), Carbon-13 constraints on the seasonal inorganic carbon budget at the BATS site in the northwestern Sargasso Sea, *Deep-Sea Res. I*, *45*, 673–717.
- Gruber, N., C. D. Keeling, R. B. Bacastow, P. R. Guenther, T. J. Lueker, M. Wahlen, H. A. J. Meijer, W. G. Mook, and T. F. Stocker (1999), Spatiotemporal patterns of carbon-13 in the global surface oceans and the oceanic Suess effect, *Global Biogeochem. Cycles*, *13*, 307–335.
- Gruber, N., C. D. Keeling, and N. Bates (2002), Interannual variability of the North Atlantic Ocean carbon sink, *Science*, *298*, 2374–2378.
- Gruber, N., P. Friedlingstein, C. B. Field, R. Valentini, M. Heimann, J. E. Richey, P. Romero-Lankao, D. Schulze, and C. Chen (2004), The vulnerability of the carbon cycle in the 21st century: An assessment of carbon-climate-human interactions, in *Toward CO₂ stabilization: Issues, Strategies, and Consequences*, edited by C. B. Field and M. R. Raupach, chap. 2, Island Press, Vienna.
- Hare, S. R., and N. J. Mantua (2000), Empirical evidence for North Pacific regime shifts in 1977 and 1989, *Progress in Oceanography*, *47*(2-4).
- Heimann, M. (1995), Dynamics of the carbon cycle, *Nature*, *375*, 629–630.
- Houghton, J. T., Y. Ding, D. J. Griggs, M. Noguer, P. J. van der Linden, X. Dai, K. Maskell, and C. A. Johnson (Eds.) (2001), *Climate Change 2001: The Scientific Basis. Contribution of Working Group I to the Third Assess-*

- ment Report of the Intergovernmental Panel on Climate Change, Cambridge University Press, New York.
- Karl, D. M., R. Letelier, L. Tupas, J. Dore, J. Christian, and D. Hebel (1997), The role of nitrogen fixation in the biogeochemical cycling in the subtropical North Pacific Ocean, *Nature*, **388**, 533–538.
- Karl, D. M., and R. Lukas (1996), The Hawaii Ocean Time-series (HOT) program: Background, rationale and field implementation, *Deep-Sea Res. II*, **43**(2-3), 129–156.
- Karl, D. M., R. Letelier, D. Hebel, L. Tupas, J. Dore, J. Christian, and C. Winn (1995), Ecosystem changes in the North Pacific subtropical gyre attributed to the 1991-92 El Niño, *Nature*, **373**, 230–234.
- Karl, D. M., J. R. Christian, J. E. Dore, D. V. Hebel, R. M. Letelier, L. M. Tupas, and C. D. Winn (1996), Seasonal and interannual variability in primary production and particle flux at Station ALOHA, *Deep-Sea Res. II*, **43**(2-3), 539–568.
- Kawamura, R. (1994), A rotated EOF analysis of global sea surface temperature variability with interannual and interdecadal scales, *J. Phys. Oceanogr.*, **24**, 707–715.
- Keeling, C. D., R. B. Bacastow, A. F. Carter, S. C. Piper, T. P. Whorf, M. Heimann, W. G. Mook, and H. Roelofzen (1989), A three dimensional model of atmospheric CO₂ transport based on observed winds: 1. analysis of observational data, in *Aspects of Climate Variability in the Pacific and the Western Americas*, edited by D. H. Peterson, Geophys. Monogr. Ser., **55**, pp. 165–237, AGU, Washington, D.C.
- Keeling, C. D., T. P. Whorf, M. Wahlen, and J. van der Plicht (1995), Interannual extremes in the rate of rise of atmospheric carbon dioxide since 1980, *Nature*, **375**, 666–670.
- Keeling, C. D., H. Brix, and N. Gruber (2004), Seasonal and long-term dynamics of the upper ocean carbon cycle at station ALOHA near Hawaii, *Global Biogeochem. Cycles*, in press.
- Kindermann, J., G. Würth, G. H. Kohlmaier, and F.-W. Badeck (1996), Interannual variation of carbon exchange fluxes in terrestrial ecosystems, *Global Biogeochem. Cycles*, **10**(4), 737–755.
- Laws, E. A., P. G. Falkowski, J. Smith, W. O., H. Ducklow, and J. J. McCarthy (2000), Temperature effects on export production in the open ocean, *Global Biogeochem. Cycles*, **14**(4), 1231–1246.
- Le Quéré, C., J. C. Orr, P. Monfray, O. Aumont, and G. Madec (2000), Interannual variability of the oceanic sink of CO₂ from 1979 through 1997, *Global Biogeochem. Cycles*, **14**, 1247–1265.
- Lomas, M. W., N. R. Bates, A. H. Knap, D. M. Karl, R. Lukas, M. R. Landry, R. R. Bidigare, D. K. Steinberg, and C. A. Carlson (2002), Refining our understanding of oceanic biogeochemistry and ecosystem functioning, *EOS, Transactions, Am. Geophys. Union*, **83**(48), 559–567.
- Lukas, R., and D. Karl (1999), Hawaii Ocean Time-series (HOT), 1988-1998: A decade of interdisciplinary oceanography, *Tech. Rep. 99-05*, CD-ROM, School of Ocean and Earth Science and Technology, University of Hawaii, updates at URL: <http://hahana.soest.hawaii.edu/hot/hot.html>.
- Mantua, N. J., and S. R. Hare (2002), The Pacific Decadal Oscillation, *Journal of Oceanography*, **58**(1), 35–44.
- Mantua, N. J., S. R. Hare, Y. Zhang, J. M. Wallace, and R. C. Francis (1997), A pacific interdecadal climate oscillation with impacts on salmon production, *Bull. Am. Meteorol. Soc.*, **78**(6), 1069–1079.
- McGowan, J. (1995), HOT and the North Pacific gyre, *Nature*, **378**, 21–22.
- McKinley, G. A. (2002), Interannual variability of air-sea fluxes of carbon dioxide and oxygen, Ph.D. thesis, Massachusetts Institute of Technology.
- McKinley, G. A., M. J. Follows, and J. Marshall (2004), Mechanisms of air-sea CO₂ flux variability in the equatorial Pacific and the North Atlantic, *Global Biogeochem. Cycles*, **18**(2), GB2011, doi:10.1029/2003GB002179.
- McPhaden, M. J. (1999), Genesis and evolution of the 1997–98 El Niño, *Science*, **283**(5404), 950–954.
- Michaels, A. F., and A. H. Knap (1996), Overview of the U.S. JGOFS Bermuda Atlantic Time-series Study and the Hydrostation S program, *Deep-Sea Res. II*, **43**(2-3), 157–198.
- Miller, A. J., and N. Schneider (2000), Interdecadal climate regime dynamics in the North Pacific Ocean: theories, observations and ecosystem impacts, *Progress in Oceanography*, **47**(2-4), 355–379.
- Peterson, W. T., and F. B. Schwing (2003), A new climate regime in northeast pacific ecosystems, *Geophys. Res. Lett.*, **30**(17), 1896, doi:10.1029/2003GL017528.
- Peylin, P., P. Bousquet, C. Le Quéré, P. Friedlingstein, S. Sitch, G. McKinley, N. Gruber, P. Ciais, and P. Rayner (2004), Interannual CO₂ fluxes as deduced by inverse modeling and by models of the biogeochemical carbon cycle, *Global Biogeochem. Cycles*, in press.
- Philander, S. G. (1990), *El Niño, La Niña, and the Southern Oscillation*, Academic Press, 293 pp.
- Plattner, G.-K., F. Joos, T. F. Stocker, and O. Marchal (2001), Feedback mechanisms and sensitivities of ocean carbon uptake under global warming, *Tellus, Ser. B.*, **53**, 564–592.
- Quay, P. (2002), Ups and downs of CO₂ uptake, *Science*, **298**, 2344.
- Quay, P., and J. Stutsman (2003), Surface layer carbon budget for the subtropical N. Pacific: d¹³C constraints at Station ALOHA, *Deep-Sea Res. I*, **50**(9), 1045–1061, doi: 10.1016/S0967-0637(03)00116-X.
- Rasmusson, E., and T. Carpenter (1982), Variations in the tropical sea surface temperature and surface wind fields associated with the Southern Oscillation/El Niño, *Mon. Wea. Rev.*, **110**, 354–384.
- Rayner, P., I. Enting, R. Francey, and R. Langenfelds (1999), Reconstructing the recent carbon cycle from atmospheric CO₂, δ¹³C and O₂/N₂ observations, *Tellus, Ser. B.*, **51B**, 213–232.
- Rödenbeck, C., S. Houweling, M. Gloor, and M. Heimann (2003), Time-dependent atmospheric CO₂ inversions based

- on interannually varying tracer transport, *Tellus*, 55B, 488–497.
- Rubinstein, R. Y. (1981), *Simulation and the Monte Carlo method*, John Wiley & Sons, New York.
- Sarmiento, J. L., and N. Gruber (2002), Sinks for anthropogenic carbon, *Physics Today*, 55(8), 30–36.
- Sarmiento, J. L., T. M. C. Hughes, R. J. Stouffer, and S. Manabe (1998), Simulated response of the ocean carbon cycle to anthropogenic climate warming, *Nature*, 393, 245–249.
- Sitch, S., et al. (2003), Evaluation of ecosystem dynamics, plant geography and terrestrial carbon cycling in the LPJ dynamic global vegetation model, *Global Change Biology*, 9(2), 161–185.
- Sonnerup, R. E., P. D. Quay, and J. L. Bullister (1999), Thermocline ventilation and oxygen utilization rates in the subtropical North Pacific based on CFC distributions during WOCE, *Deep-Sea Res. I*, 46(5), 777–805.
- Sprintall, J., and M. Tomczak (1992), Evidence of the barrier layer in the surface layer of the tropics, *J. Geophys. Res.*, 97(C5), 7305–7316.
- Steinberg, D. K., C. A. Carlson, N. R. Bates, S. A. Goldthwait, L. P. Madin, and A. F. Michaels (2000), Zooplankton vertical migration and the active transport of dissolved organic and inorganic carbon in the Sargasso Sea, *Deep-Sea Res. I*, 47(1), 137–158.
- Takahashi, T., et al. (2002), Global sea-air CO₂ flux based on climatological surface ocean pCO₂, and seasonal biological and temperature effects, *Deep-Sea Res. II*, 49(9–10), 1601–1622.
- Williams, P. J. I. (1993), On the definition of plankton production terms, *ICES Mar. Sci. Symp.*, 197, 9–19.
- Winguth, A. M. E., M. Heimann, D. Kurz, E. Maier-Reimer, U. Mikolajewicz, and J. Segschneider (1994), El Niño–Southern Oscillation related fluctuations of the marine carbon cycle, *Global Biogeochem. Cycles*, 8(1), 39–63.
- Winn, C. D., Y.-H. Li, F. T. Mackenzie, and D. M. Karl (1998), Rising surface ocean dissolved inorganic carbon at the Hawaii Ocean Time-series site, *Mar. Chem.*, 60(1–2), 33–47.

H. Brix, N. Gruber, Department of Atmospheric and Oceanic Sciences & IGPP, 3845 Slichter Hall, UCLA, Los Angeles, CA 90095-1567 (hbrix@igpp.ucla.edu; ngruber@igpp.ucla.edu)

C. D. Keeling, Scripps Institution of Oceanography, University of California, San Diego, La Jolla, CA 92093-0220. (cdkeeling@ucsd.edu)